CHARACTERIZATION OF A DATA ACQUISITION SYSTEM IN A REMOTELY CONTROLLED ENVIRONMENT

P.Carbone, E.Nunzi, D.Petri

Dipartimento di Ingegneria Elettronica e dell'Informazione,
Università degli Studi di Perugia, via G.Duranti 93 – 06125 Perugia, Italy.
Phone: ++39 075 5853629, Fax: ++39 075 5853654, e-mail: carbone@diei.unipg.it

Abstract – *Parameters estimation of a data acquisition system can be performed by using several estimation algorithms. The choice of the most appropriate test method is not straightforward, but it depends on both the type of the converter under test and on the parameters to be measured. Moreover, various test methods and algorithms may present different sensitivities to noise and system parameter's variations, thus resulting in diverse estimation accuracies. In this paper, the number of effective bits of a commercial 16-bit acquisition system has been evaluated by using a remotely controlled environment based on the network. Experimental data obtained by using the code density and a frequency domain based test techniques are presented and compared with published theoretical results. It is shown that a suitable choice of the procedure parameters allows optimum exploitment of available measurement resources.*

Keywords – Frequency Domain Test Method, Histogram Test Method, Remotely Controlled Data Acquisition System.

1. INTRODUCTION

In the last decade, the rapid evolution of both digital integrated circuit technologies and network communications systems has led to new approaches in the design and employment of measurement and electronic systems. The numerous architectures based on digital signal processing of numerical data and on the development of virtual instrumentation technologies, substantially changed the procedural methods applied when taking measurements. As a result, the characterization of an electronic system often requires a thorough understanding of analog and digital electronic issues along with knowledge of virtual instrumentation basics.

Most of the electronic instruments used in an industrial environment or in a measurement laboratory, both ordinary and virtual, present a system architecture based on a data acquisition block consisting in an analog-to-digital converter (ADC) followed by digital processing of the acquired data. Since its features heavily affect the measurement system performance, the metrological characterization of the conversion system has a key relevance.

In [1]–[6], techniques for the characterization of ADCs test procedures, both in the amplitude and in the frequency domains, are considered and main parameters characterizing such measurement algorithms are determined. Suggestions about the practical realization of such testing techniques are given in the IEEE standards 1057 [3] and 1241 [7]. Such documents recommend the use of coherent sampling in order to maximize the accuracy of the estimated parameters. However, because of inaccuracies in the analog circuitry of the conversion system, the ADC output spectrum can be affected by spurious components which can not be sampled coherently. Such phenomenon is critical when evaluating most ADC figures of merit in the frequency-domain such as signal-to-random noise ratio ($SRNR$), signal-to-non-harmonic ratio ($SNHR$), or signal-to-noise and distortion ratio ($SINAD$) because the algorithm requires the estimation of the wide-band noise level and of the amplitude of each narrowband component included in the ADC output spectrum. As it is well known, non-coherent sampling requires the adoption of data windowing in order to reduce spectral leakage effects.

With the aim of verifying the accuracy of the testing techniques in the amplitude and in the frequency domain, the algorithms described in [1]–[6] have been applied for the measurement of the number of effective bits of a commercial 16 bit-20ksamples/s acquisition board subjected to a single tone stimulus. The testing procedures have been performed by using a remotely controlled measurement set-up based on the Transmission Control Protocol / Internet Protocol (TCP/IP) data transmission system and the acquired data have undergone processing by using both the code density test and a discrete Fourier transform (DFT) based algorithm [1] [4] [5].

In particular, DFT-windowing has been performed using windows belonging to the cosine class which approximate the zero-order Discrete Prolate Spheroidal Sequences (DPSS). These sequences are known to optimize the leakage/mainlobe trade-off and, consequently, maximize the accuracy of the wide-band noise estimator [2]. The use of the cosine windows has been preferred over that of the DPSS because of the lower computational effort in determining its samples values.

After briefly introducing both testing procedures, the measurement bench set-up used for acquiring data is described. Estimates of the effective number of bits obtained by applying the two techniques are then compared in order to validate both testing procedures. Results, presented in section 3, show that a careful choice of both algorithms parameters allows a good estimation of the characteristic of the system under test.

2. ESTIMATION OF THE NUMBER OF EFFECTIVE BITS

With the aim of verifying the effectiveness of the ADC testing procedures based on the code density and on the DFT tests, a sinewave source exhibiting adequate spectral purity has been employed to stimulate the data acquisition board. Then, the number of effective bits has been measured under several testing conditions. This is a parameter which describes the overall performance of a conversion system and which can be esti-

ISBN 972-98115-5-5

mated by independently applying either one of the techniques.

In the next two subsections are described the fundamental principles for the estimation of the number of effective bits of a data acquisition system by means of both techniques.

2.1 Histogram test based procedure

The testing procedure based on the histogram method provides the estimates of each transition level by means of the cumulative histogram of the converter output codes [6]. The number of effective bits, b_e, can then be determined by:

$$b_e = b - \frac{1}{2}\log_2\left(\frac{\mathrm{mse}}{\Delta^2/12}\right) \tag{1}$$

where b is the nominal number of bit of the acquisition board, Δ is the quantization step of the internal ADC and mse is the ADC output mean square error corresponding to a uniformly distributed input. Such quantity, evaluated by stimulating all converter output codes, has the following expression [5]:

$$\mathrm{mse} = \frac{\Delta^2}{12} + \frac{1}{N}\sum_{k=1}^{N-1}\mathrm{inl}_k^2 + \sigma_\eta^2, \tag{2}$$

in which $N \triangleq 2^b$, σ_η^2 represents the variance of the input-equivalent noise source and $\mathrm{inl}_k, k = 1, ..., N$ is the k-th integral non linearity. The estimation of such inl's has been carried out by following directions suggested in [7], i.e. taking various records of sinewave data. However, because of additive noise and since finite record length are considered, the estimation of the k-th inl is affected by an error ε_k. As a result, the estimation of the mse, $\widehat{\mathrm{mse}}$, can be written as:

$$\widehat{\mathrm{mse}} = \frac{\Delta^2}{12} + \frac{1}{N}\sum_{k=1}^{N-1}\widehat{\mathrm{inl}}_k^2, \tag{3}$$

where $\widehat{\mathrm{inl}}_k$ is an estimator of inl_k. It has been demonstrated that by taking a sufficiently high number of samples, the expected value of (3), $\overline{\mathrm{mse}}$, satisfies the following relationship [5]:

$$\overline{\mathrm{mse}} \triangleq E\left[\widehat{\mathrm{mse}}\right] \simeq \frac{\Delta^2}{12} + \frac{1}{N}\sum_{k=1}^{N-1}\mathrm{inl}_k^2. \tag{4}$$

Equation (4) shows that the histogram test corrects the effect of the converter input-referred wide-band noise [5], thus taking into account only the deterministic behavior of the system. If $\widehat{b}_e$ represents the estimated number of effective bits, by substituting (4) in (1) we have:

$$\overline{b}_e \triangleq E\left[\widehat{b}_e\right] \simeq b - \frac{1}{2}\log_2\left(\frac{\overline{\mathrm{mse}}}{\Delta^2/12}\right). \tag{5}$$

Experimental data, presented in section 3, have been derived by stimulating the board under test with a sinewave source. In particular, in order to obey the coherency condition [9], the sinewave input frequency, f_{in}, has been chosen so that:

$$\frac{f_{in}}{f_s} = \frac{D}{M} \tag{6}$$

is satisfied, where f_s is the board sampling frequency, M is the number of acquired samples and D is an integer number relatively prime with M. This condition concurs to extract the maximum information from the acquired data thus assuring the maximum efficiency of the histogram test.

2.2 Frequency domain based procedure

Since non-coherent sampling is assumed, the frequency domain based procedure requires windowing of data samples by means of a suitable sequence, $w[\cdot]$. Then, the number of effective bits, b_e, is estimated as follows [2]:

$$\widehat{b}_e = \frac{1}{2}\log_2\left(\frac{2}{3}\widehat{SRNR}\right) \tag{7}$$

where $\widehat{SRNR}$ is the estimated signal to random noise ratio. By defining $\widehat{\sigma}_R^2$ and $\widehat{\sigma}_X^2$ as the power estimators of the output-referred wide-band noise and of the input sinewave, respectively, we have [2]:

$$\widehat{SRNR} = \frac{N_R}{N_R + \mathrm{ENBW}_0}\frac{\widehat{\sigma}_X^2}{\widehat{\sigma}_R^2} \tag{8}$$

$$\widehat{\sigma}_R^2 \triangleq \frac{1}{N_R N_s^2}\frac{1}{\mathrm{NNPG}}\sum_{k\in\mathcal{B}_\mathcal{R}}|Y[k]|^2 \tag{9}$$

$$\widehat{\sigma}_X^2 \triangleq \frac{2}{N_s^2}\frac{1}{\mathrm{NNPG}}\sum_{k\in\mathcal{B}_X}|Y[k]|^2 - 2\frac{N_X}{N_s}\widehat{\sigma}_R^2. \tag{10}$$

In (8), (9) and (10) N_s is the number of acquired samples, $Y[\cdot]$ is the windowed DFT (WDFT) of the acquired data samples, N_X is the cardinality of $\mathcal{B}_X$, the interval of frequency bins in which the energy of the fundamental component is mostly confined and N_R is the cardinality of $\mathcal{B}_\mathcal{R}$, the set of frequency bins whose energy is mostly due to the wide-band noise. Moreover, $\mathrm{NNPG} \triangleq \frac{1}{N}\sum_{n=0}^{N-1} w^2[n]$ is the window Normalized Noise Power Gain and $\mathrm{ENBW}_0 \triangleq \sum_{n=0}^{N_s-1} w^4[n]/(\sum_{n=0}^{N_s-1} w^2[n])^2$ represents the equivalent-noise bandwidth of the squared window. Notice that the factor $N_R/(N_R + \mathrm{ENBW}_0)$ in (8) is introduced in order to correct for a bias contribution due to (9).

It is shown in (App. A) that, the variance of (7) can be written as:

$$\mathrm{var}\{\widehat{b}_e\} \simeq 0.5\frac{\mathrm{ENBW}_0}{N_R}. \tag{11}$$

With the aim of maximizing the accuracy of expressions (8)–(10), a suitable window sequence must be chosen.

It has been demonstrated that the zero-order DPSS are windows maximizing the accuracy of the noise estimator [2]. However, the procedure for calculating the value of such window samples is complicated, because it depends on the window length, i.e. on the number of acquired data samples N_s, and, in addition, it is not available a closed form for its computation. The windows $w[\cdot]$ employed in this paper are those

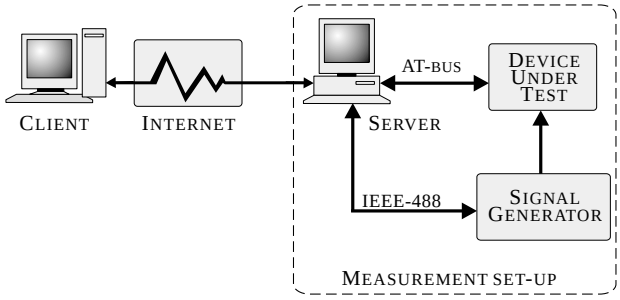

Figure 1. Remote control system of the measurement set-up employed in the characterization of the AT-MIO-16XE-50 board.

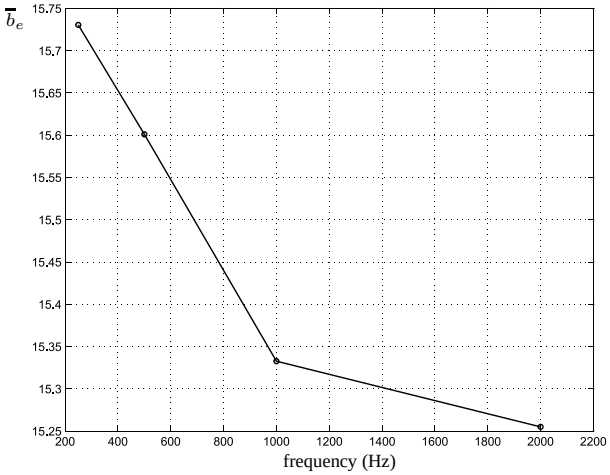

Figure 2. Number of effective bit of the AT-MIO-16XE-50 acquisition board estimated by means of the histogram test method for four different values of the sinewave input frequency.

attaining to the cosine-class windows, i.e.

$$w[n] \triangleq \sum_{i=0}^{H-1} (-1)^i a_i \cos\left(2\pi n \frac{H}{N}\right), \quad n = 0, ..., N_s - 1 \quad (12)$$

where a_i are the window coefficients and H is the number of such coefficients.

Samples of these windows are evaluated more easily with respect to those of the first order DPSS, since they are completely determined by the window coefficients independently from the length of the acquired record. In particular, the coefficients used for this test, reported in Tab. I, are those obtained from a minimization, in the least mean square sense, of the difference between the DPSS related to a given the mainlobe width, Λ. More specifically, the minimization has been carried out by choosing the number of coefficients $H = \lceil \Lambda \rceil + 1$, in which $\lceil x \rceil$ returns the last integer greater than or equal to x. Being the zero-order DPSS the sequences characterized by minimum leakage for a given mainlobe width, this choice generates low spectral-leakage windows.

3. MEASUREMENTS BENCH SET-UP AND EXPERIMENTAL RESULTS

Test procedures presented above have been automated and inserted in a remotely controlled environment, realized in Labview™, which make use of the TCP/IP protocol. The block scheme of the system employed to manage the measurement set-up is shown in Fig. 1. More specifically, the device under test is the AT-MIO-16XE-50, a 16 bit data acquisition board, developed by National Instrument, internally placed on the AT-bus of the server. Such a board is characterized by a sampling frequency of 20 ksamples/s and four full scale ranges equal to ± 0.1 V, ± 1 V, ± 5 V and ± 10 V. Moreover, the signal generator used for stimulating the board is the SRS DS360, a function generator exhibiting an SFDR larger than 96dBc, controlled by the server using the IEEE-488 bus.

In such a configuration, the client preliminarily defines the kind of test to be performed and then settles the signal generator and acquisition board parameter values, such as the full scale range (FS), the frequency and amplitude (A) of the input signal, the board sampling rate, the number of acquired data records (N_{REC}), the length of each record and, for the DFT approach, the window to be used. After that, the client opens a TCP/IP connection towards the server, which configures the board under test together with the signal generator and acquires the data provided by the board. The software processing data has been written so that the parameter estimation algorithm runs on the server, while the client receives the estimated value. This choice has been preferred over that of processing all the acquired data on the client in order to lower the amount of data to be transferred through the Internet network.

The number of effective bits obtained by means of the histogram and energy test methods are shown in Fig. 2 and Fig. 4, respectively.

Estimations derived by applying the histogram test method have been achieved by varying the frequency of the input sinewave and by setting the full-scale range of the board and the sinewave amplitude to 10 V. The set of frequencies employed for the measurement reported in Fig. 2 are: 250.14 Hz, 500.38 Hz, 1000.18 Hz, 2000.46 Hz, which satisfy the coherent sampling condition (6). In particular the number of integer sinewave cycles D, which correspond to each of the previous frequency values, are: 12507, 25019, 50009, 106151, respectively. Measurements have then been carried out by averaging 10 records of 10^6 samples each. The behavior reported in Fig. 2 shows that the number of estimated effective bits is lower as higher the stimulating frequency, accordingly with considerations presented in [7] and [9].

Estimations obtained by applying the frequency domain method have been derived by using a sinewave at 1 kHz, by setting the full-scale range of the board to 10 V and by varying the mainlobe width of the cosine windows. Measurements have been carried out by averaging 100 records of 16384 data samples each and by choosing N_X equal to $2M + 1$, as suggested in [2].

In order to determine the most appropriate sinewave amplitude to be employed, the board under test has been stimulated with sinewave amplitudes ranging from 9.7 V to 10 V (the input full scale of the board) and by employing a cosine window with $\Lambda = 4.9$ bin, which is an almost optimum value accordingly with indications presented in [2].

TABLE I

Λ	a_0	a_1	a_2	a_3	a_4	a_5	a_6
3.1	0.40160665815193	0.49783275179051	0.09896225998909	0.00148531354322	0.00011301652525		
3.4	0.38347646457116	0.49506956596406	0.11674912760303	0.00466283792247	0.00004200393927		
3.9	0.35805595361695	0.48796100461854	0.14199942427928	0.01197823491213	0.00000538257310		
4.1	0.34921948772871	0.48458308120712	0.15072452230112	0.01538577242381	0.00008701441586	0.00000012192338	
4.4	0.33710407020498	0.47916437381384	0.16251026228077	0.02082094638200	0.00039796256061	0.00000238475779	
4.7	0.32616819716606	0.47349099254870	0.17289753192519	0.02650388143189	0.00093901340984	0.00000038351833	
4.8	0.32275262461523	0.47156554158576	0.17607798442412	0.02843060102615	0.00117235791474	0.00000089043399	
4.9	0.31944276487758	0.46963026227408	0.17912743899447	0.03036684069241	0.00143221631651	0.00000047684494	
5.0	0.31623276538022	0.46768748853130	0.18205102710991	0.03230903329888	0.00171836944541	0.00000131623428	
5.1	0.31311730091924	0.46573942435705	0.18485372502210	0.03425392880704	0.00203047544679	0.00000495535692	0.00000019009087
5.2	0.31009223805483	0.46378923241848	0.18754079182545	0.03619865723896	0.00236809343577	0.00001090711681	0.00000007990970
5.7	0.29618077682821	0.45407341002197	0.19940150417023	0.04583534188641	0.00441796495044	0.00009099256247	0.00000000958027

Coefficients of the cosine window, employed in the energy based test method, which approximate the DPSS sequences for the indicated Λ.

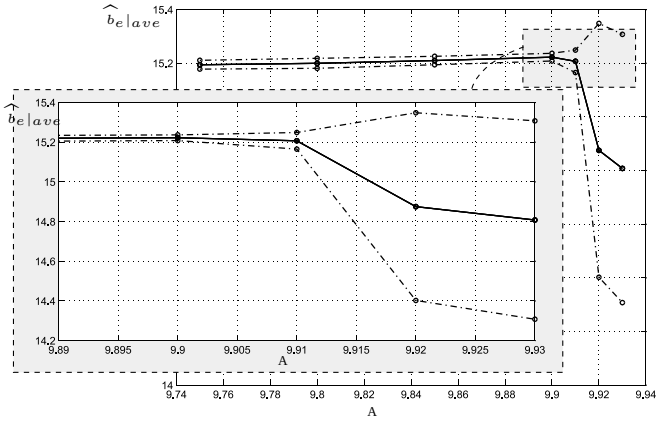

Figure 3. Number of effective bit of the AT-MIO-16XE-50 acquisition board estimated by means of the energy based test method versus the input sinewave amplitude (A) on 100 records of data. Bolded line represents the average of the measurements ($\widehat{b}_e|_{ave}$). Dashed-dot lines represent $\widehat{b}_e|_{ave}$ plus and minus the standard deviation of the measurements on 100 records of data. The gray box shows the zoom of data for values of A ranging from 8.89 V to 9.93 V. The used input sinewave frequency, f_{in}, is equal to 1 kHz.

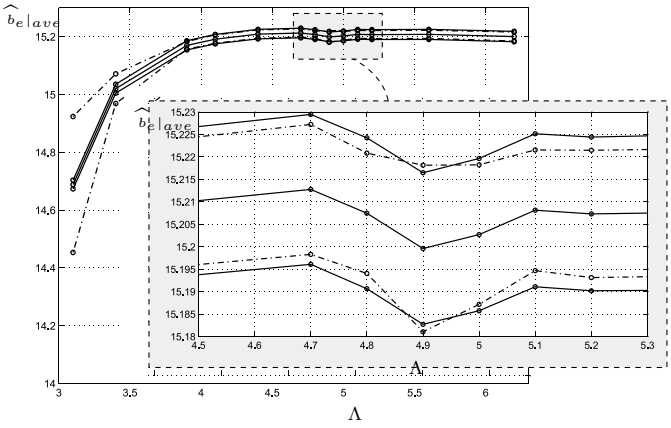

Figure 4. Number of effective bit of the AT-MIO-16XE-50 acquisition board estimated by means of the energy based test method for different choices of the cosine window main-lobe width Λ on 100 records of data. The used input sinusoidal amplitude and frequency f_{in} are equal to 9.8 V and 1 kHz, respectively. Bolded line represents the average of the measurements $\widehat{b}_e|_{ave}$. Dashed-dot lines represent $\widehat{b}_e|_{ave}$ plus and minus the standard deviation of the measurements. Solid lines represent $\widehat{b}_e|_{ave}$ plus and minus the theoretical standard deviation. The gray box shows the zoom of data for values of Λ ranging from 4.5 to 5.3 bin.

The achieved results are graphed in Fig. 3. In particular the bolded line represents the average of the estimated effective bits ($\widehat{b}_e|_{ave}$) evaluated on N_R records, while dashed-dotted lines represent $\widehat{b}_e|_{ave}$ plus and minus the standard deviation on the N_R measurements. The behavior of the curves shows that the estimation of the effective bits grows with the amplitude until the input reaches 9.9 V, the value over which the internal ADC exhibits saturation phenomena. As a consequence, the variance of the estimator (9) becomes so large that affects the estimation of the number of effective bits [1]. In order to assure the non overloading condition of the internal converter, experimental results have been obtained by setting the sinewave amplitude to 9.8 V. It should be noticed that the choice of a driving signal amplitude equal to 9.8 V over that of 9.9 V, lowers the number of the estimated effective bits of a quantity equal to 0.015, which is negligible with respect to the measurements accuracy.

By employing such setup settings, the frequency domain test method have been applied by varying the window main-lobe width from 2.9 to 6.2 bin and results are shown in Fig. 4. The bolded line graphed in such a figure represents $\widehat{b}_e|_{ave}$, dashed-dot lines represent $\widehat{b}_e|_{ave}$ plus and minus the standard deviation and solid lines represent $\widehat{b}_e|_{ave}$ plus and minus the theoretical standard deviation, which is derived by calculating the root mean square of (11). The behavior of experimental results shows that if the mainlobe width Λ is sufficiently large, then the frequency domain based algorithm turns out estimation values which are similar to those obtained with the histogram test, thus validating the accuracy of both test methods.

In addition Fig. 4 shows that when Λ is sufficiently high (larger than 4 bin), the standard deviation of the estimations is almost equal to that provided by the theory. When Λ is larger than 4.9 bin, estimated values do not increase significantly. Moreover, a larger Λ reduces the frequency selectivity of the algorithm and increases the standard deviation of the estimates, as provided by (11).

On the contrary, by setting a lower value for Λ, the spec-

tral leakage phenomenon becomes relevant thus affecting the estimation of the broad-band noise. Data reported in Fig. 4 clearly shows that the higher the window leakage (i.e. the lower the mainlobe width) the larger the estimation accuracy, as described in [1]. More specifically it has been experimentally verified that, the choice of windows with Λ lower than 2.9 leads to a non-significant results.

Figures (2) and (4) show that the $\widehat{b}_e$ estimates provided by the histogram method are always higher than that evaluated by using the energy based method (at least a tenth of bit). It should be noticed, however, that the histogram test provides the estimates of the number of effective bits by taking into account also the device non-linearity. In order to properly compare results obtained from the two techniques, the number of effective bits which represents the $SINAD$ has been estimated by applying the frequency domain method to the same set of data used for deriving the $SRNR$. The achieved estimates present a behavior similar to that resulting in Fig. 4 and values of about 0.4 bits less. Thus, the number effective bits obtained by applying the histogram test results to be higher than that provided by the frequency-domain approach of a quantity about equal to 0.5 bits. This is due to the fact that the histogram take the average of the wide-band noise, thus considering only the deterministic behavior of the conversion system [5] [7].

CONCLUSIONS

In this paper both the histogram and the frequency-domain based test procedures have been applied to a commercial 16 bit acquisition board remotely controlled by the TCP/IP data transmission protocol. The number of effective bits estimated by using the two techniques differs of about half a bit. In particular the number of bits estimated by means of the histogram test results to be higher because it averages the effect of the converter input-referred wide-band noise.

The frequency-domain based algorithm has been also applied to the board under test. Experimental results shows that the choice of the cosine-class windows which approximate the zero-order DPSS allows to achieve a good estimation of the parameter of interest because of the low window leakage. In addition it has been verified experimentally that when the chosen window exhibits a sufficiently large mainlobe width, the standard deviation of the effective bit estimated by applying the frequency-domain based method is almost equal to that provided by the theory.

APPENDIX A

DERIVATION OF EXPRESSION (11)

It has been demonstrated in [1] that expression of the variance of (8) is:

$$\mathrm{var}\{\widehat{SRNR}\} \simeq \frac{\mathrm{ENBW}_0}{N_R} SRNR_{id}^2 \qquad \text{(A.1)}$$

in which $SRNR_{id}$ is the signal-to-noise ratio corresponding to the nominal number of resolution bits.

By applying a first-order differential analysis to (7), the following results:

$$\mathrm{var}\{\widehat{b}_e\} \simeq \left(\frac{d\widehat{b}_e}{d\widehat{SRNR}}\right)^2 \mathrm{var}\{\widehat{SRNR}\} \simeq 0.5\frac{\mathrm{ENBW}_0}{N_R} \qquad \text{(A.2)}$$

REFERENCES

[1] P.Carbone, D.Petri, "Effective Frequency-Domain ADC Testing," *IEEE Trans. on Circ. and Sys.–II: Analog and Digital Signal Processing*, vol. 47, no. 7, pp. 660–663, July 2000.

[2] M. Bertocco, P.Carbone, E.Nunzi, D.Petri, "Windows for ADC Dynamic Testing via Frequency-domain analysis," *17th Instrumentation and Measurement Tech. Conf.*, vol. 1, pp. 114–118, Baltimore (US), May 1–4, 2000.

[3] *Standard for Digitizing Waveform Recorders*, IEEE Std. 1057, Dec. 1994.

[4] European Project DYNAD, "Methods and draft standards for the DYNamic characterisation and testing of Analogue to Digital converters," published in internet at *http://www.fe.upt.pt/~hsm/dynad*.

[5] P.Carbone, D.Petri, "Noise Sensitivity of the ADC Histogram Test," *IEEE Trans. on Instr. and Meas.*, vol. 47, no. 4, pp. 1001–1004, Aug 1998.

[6] J. Blair, "Histogram measurement of ADC nonlinearities using sinewaves," *IEEE Trans. on Instr. and Meas.*, vol. 43, pp. 373-383, June 1994.

[7] *Standard for Terminology and Test Methods for Analog- to-Digital Converters*, IEEE Std 1241 DRAFT, Oct. 2000.

[8] ENV 13005:1999, *Guide to the Expression of Uncertainty in Measurement*.

[9] P.Carbone, G.Chiorboli, "ADC Sinewave Histogram Testing with Quasi-coherent Sampling" accepted for publication in *IEEE Trans. on Instr. and Meas.*